Journal of Structural Geology 35 (2012) 51–63

Contents lists available at SciVerse ScienceDirect

Journal of Structural Geology

journal homepage: www.elsevier.com/locate/jsg

Fault inversion *vs.* new thrust generation: A case study in the Malargüe fold-and-thrust belt, Andes of Argentina

José F. Mescua*, Laura B. Giambiagi

IANIGLA, CCT Mendoza, CONICET, Av. Ruiz Leal s/n, Parque General San Martín, Apartado Postal: 330, 5500 Mendoza, Argentina

ARTICLE INFO

Article history:
Received 15 August 2011
Received in revised form
15 November 2011
Accepted 19 November 2011
Available online 29 November 2011

Keywords:
Fault inversion
Malargüe fold-and-thrust belt
Andes
Numerical modeling

ABSTRACT

The reverse reactivation of pre-existing normal faults has been documented in many orogens. In other cases, the lack of sub-surface information has allowed the construction of both inversion and non-inversion structural models. We will analyze the possibility of fault inversion in one such case, in the Malargüe fold-and-thrust belt in the Andes of Argentina. In order to address this issue, we modeled fault inversion vs. new thrust generation using the ReActiva 2.4 software, and varying the physical parameters for the pre-existing fault and the host rock. The results of modeling are compared to the possible sub-surface characteristics of faults in the Malargüe fold-and-thrust belt. We show that the orientation of these structures in the Andean stress field makes them likely to reactivate if the pre-existing fault planes present a low coefficient of friction and/or fluid overpressure. Both are expectable in the geological setting in which the structures are found. We conclude that fault inversion cannot be dismissed, and should be taken into account for structural models of the Malargüe fold-and-thrust belt. Our results can be extended to other orogens with similar characteristics.

1. Introduction

Structural inversion has been defined as the reversion of the dip-slip component of the original movement of basin-controlling extensional faults during compressional tectonics (Cooper et al., 1989; Williams et al., 1989). The substantial reactivation of the pre-existing fault system is a requisite to recognize inversion tectonics, although new structures such as footwall shortcut faults may form to some extent during this process (Cooper et al., 1989). The reactivation of a pre-existing plane implies that ancient structures are mechanically weaker than the surrounding rock (Rutter et al., 2001), which can be expressed for the seismogenic upper crust using the relation between the Coulomb–Navier fracture and slip criteria. Therefore, the orientation of the pre-existing plane with respect to the new stress field and the physical properties of the fault zone and the host rock define the possibility of reactivation. This takes place when slip along the fault plane requires less differential stress ($\sigma_1 - \sigma_3$) than the generation of a new fault (Sibson, 1985).

The inversion of pre-existing normal faults has been proposed in many modern and ancient compressional settings (Colletta et al., 1990; Grier et al., 1991; Homovc et al., 1995; Carrera et al., 2006; Mouthereau and Lacombe, 2006; Zanchi et al., 2006; and many others). In some cases, the exhumation of the structures or the availability of sub-surface data provided evidence to support the interpretation of inverted faults (Underhill and Paterson, 1998; Bjorklund and Burke, 2002; Kley and Monaldi, 2002; Kley et al., 2005; Ghisetti and Sibson, 2006). However, in other mountain belts, the evidence can be ambiguous and different researchers may propose different structural models for the same areas, i.e. inversion and non-inversion models (Helg et al., 2004; Butler et al., 2006). In such cases, a key issue is the inversion potential of the pre-existing structures in the compressional stress field, given their orientation and physical properties. In this paper, we will address this issue for a case study in an Andean fold-and-thrust belt (FTB), the Malargüe FTB. This belt was defined by Kozlowski et al. (1993) as the basement-involved deformation belt which constitutes the Andes of the southern half of the province of Mendoza (34°S–36°S), Argentina (Fig. 1). It is one of the foreland fold-and-thrust belts developed along the western margin of South America (Kley et al., 1999), related to subduction of the Nazca plate under the South American plate (Dewey and Bird, 1970), and was formed since the Cretaceous in the Andean orogeny (Ramos and Alemán, 2000). The basement-involved character of the deformation in the Malargüe FTB was recognized since the first geologic works carried out in the area (e.g. Gerth, 1931). In the sectors of the FTB

* Corresponding author. Tel.: +54 261 5244238; fax: +54 261 5244201.
E-mail addresses: jmescua@mendoza-conicet.gob.ar (J.F. Mescua), lgiambia@mendoza-conicet.gob.ar (L.B. Giambiagi).

0191-8141/$ – see front matter © 2011 Elsevier Ltd. All rights reserved.
doi:10.1016/j.jsg.2011.11.011

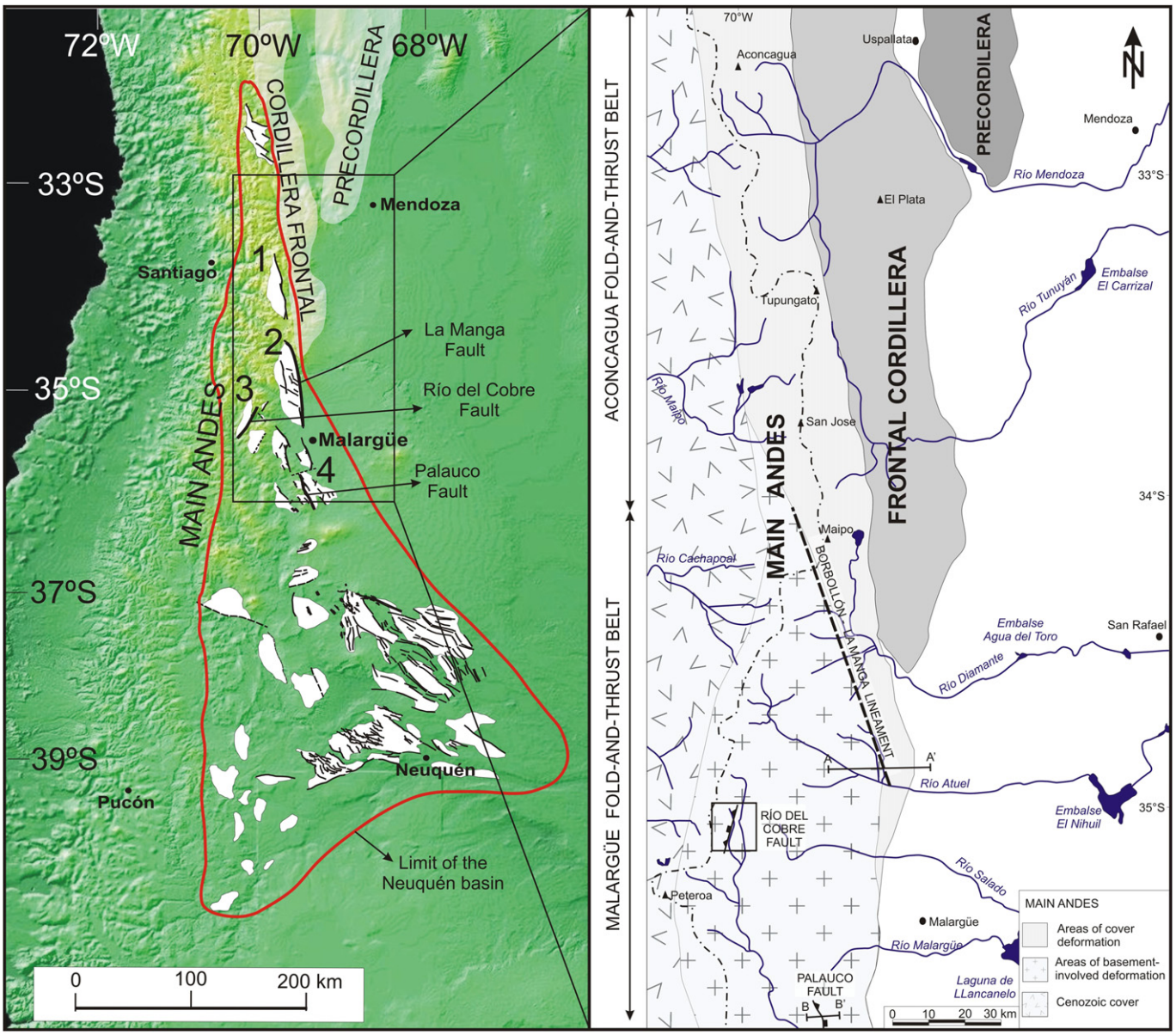

Fig. 1. Geologic setting of the Malargüe fold-and-thrust belt. (A) Regional setting. The tectonomorphic units of the Andes: Precordillera, Cordillera Frontal, Main Andes, are shown over the topography. The main extensional depocenters of the Neuquén basin are shown according to Giambiagi et al. (2009b). Note the NNW to NNE orientation of the Mesozoic normal faults in the northern sector of the basin. 1: Yeguas Muertas depocenter, 2: Atuel depocenter, 3: Río del Cobre depocenter, 4: Palauco depocenter. (B) The Andes of Mendoza, showing the location of the Aconcagua and Malargüe fold-and-thrust belts and areas of basement involved and cover deformation. The structures described in Section 5 are also shown: the Borbollón-La Manga lineament and the Río del Cobre and Palauco faults. A–A′: cross-section in Fig. 5B. B–B′: cross-section in Fig. 6.

where the basement does not crop out, its involvement in the deformation is recognized by several observations: (i) folds with large wavelengths (>5 km) limited by high-angle reverse faults, (ii) outcrops of syn-extensional Triassic and Lower to Middle Jurassic deposits, which are stratigraphically below the main detachment levels of the Mesozoic succession, (iii) variations in the structural trends which deviate from the typical N–S Andean trend. Basement involvement in the deformation in the Malargüe FTB contrasts with the deformation restricted to the Mesozoic cover of the Aconcagua FTB (Ramos et al., 1996a) developed in northern Mendoza (Fig. 1). In spite of the wide consensus about which areas in the Andes of Mendoza present basement involved and cover deformation, the mechanism of basement deformation is still a matter of debate. Two end-member structural models have been proposed: inversion (Uliana et al., 1995; Kley et al., 1999; Giambiagi et al., 2005, 2008a; Giampaoli et al., 2005) and non-inversion (Kozlowski et al., 1993; Dimieri, 1997; Turienzo, 2010) models. In inversion models, the main structures correspond to inverted Mesozoic normal faults, whereas non-inversion models attribute shortening to newly formed Andean thrusts. Intermediate "hybrid" models with both kinds of structures have also been proposed for some parts of the belt (Manceda and Figueroa, 1995; Giambiagi et al., 2009a). The lack or bad quality of sub-surface information to resolve the deep structure has allowed the development of the different structural models. Different authors have constructed balanced cross-sections using all the structural models, therefore this technique has not been able to provide a unique solution for the interpretation of the deep structure of the fold-and-thrust belt.

In order to address this controversy, we will examine the potential inversion of the Mesozoic normal faults through

numerical modeling using the ReActiva software (Tolson et al., 2001), which is based on the reformulated Coulomb–Navier criteria for non-Andersonian conditions (Yin and Ranalli, 1992). The aim of this paper is to analyze under which conditions these previous normal faults can be inverted. Modeling will be complemented with a discussion of other geological arguments for and against inversion and the analysis of particular cases of structures suspected of being inverted normal faults.

2. Fault inversion: theoretical framework

In the seismogenic upper crust, deformation in fault zones occurs by frictional processes, corresponding to brittle fracture and frictional sliding (Jaeger, 1969; Sibson, 1977; Rutter et al., 2001; Lisle and Srivastava, 2004). Sliding along a pre-existing plane occurs if the shear stress on the plane exceeds the frictional resistance (Jaeger, 1969). The reactivation of a pre-existing fault plane will take place when slip along the pre-existing plane requires less differential stress ($\sigma_1 - \sigma_3$) than the formation of a new fault in the intact rock. This in turn depends on the following factors: (1) the orientation of the plane with respect to the principal stress directions, (2) the cohesion of the pre-existing plane and host rock, (3) pore fluid pressure in the fault zone, and (4) the coefficient of friction on the plane and host rock (Jaeger, 1969; Byerlee, 1978; Sibson, 1990, 2004). The behavior of these properties is influenced by the fact that faults are not discrete surfaces but zones of finite width of fault rocks, in which specific mechanical and hydrological properties depend on a complex interplay between many factors (Wibberley et al., 2008).

The orientation of fault planes with respect to the stress field can be analyzed applying the Coulomb–Navier fracture and slip criteria. Its application is frequently carried out using the Mohr diagram (e.g. Anderson, 1951; Ramsay, 1967; Jaeger, 1969; Jaeger and Cook, 1979). A fracture envelope can be constructed on the Mohr diagram given by a pair of lines following the equation:

$$|\tau| = c + \mu\sigma_N$$

where τ is the shear stress on the plane, c is the cohesion of the material, μ is the coefficient of internal friction and σ_N is the normal stress on the plane. Similarly, a slip envelope can be constructed corresponding to the equation

$$|\tau| = c_0 + \mu_0\sigma_N$$

where c_0 is the cohesion of the pre-existing fault plane and μ_0 is the coefficient of friction of the same plane. For determinate stress conditions, the domain of slip along pre-existing planes contains all the planes that lie below the line of the Coulomb fracture criterion and above the line of the Coulomb sliding criterion (Fig. 2). In this field, the planes are stable for fracture and unstable for slip. In order to use the Mohr diagram, the data need to be transformed between stress space ($\sigma_N - \tau$ space) and physical space (Alaniz-Álvarez et al., 1998), which complicates the visualization of the planes prone to reactivation. Application of the Mohr diagram to evaluate the reactivation of faults requires specifying the physical conditions (cohesion and coefficient of friction) of the materials involved, in this case, intact rock and the pre-existing fault plane, and the magnitudes of the principal stresses, to obtain the fracture and sliding envelopes.

Regarding the physical properties of the fault plane and host rock, cohesion (c) is defined as the resistance to sliding (equal to the critical shear stress) in the absence of normal stress. It is measured

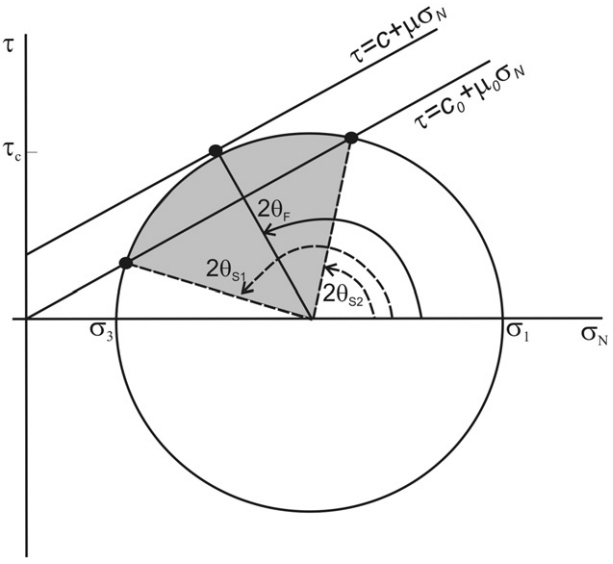

Fig. 2. Mohr diagram in 2D (for planes containing σ_2), showing the Coulomb fracture and slip envelopes for the case of a cohesionless pre-existing plane. For rocks with a cohesion c and a friction coefficient μ, τ_c is the critical shear to produce a fracture, which is produced with an angle θ_F. If the rock contains cohesionless pre-existing planes with a friction coefficient of μ_0, and oriented at angles between θ_{S1} and θ_{S2}, slip on these planes will require a smaller τ than τ_c, and reactivation will take place. Modified from Morley et al., 2004.

in units of pressure, and a compilation of values for different lithologies ranges between $c = 1$ MPa for soft sedimentary rocks to $c = 55$ MPa for hard volcanic rocks (Afrouz, 1992). On the other hand, Byerlee (1978) proved that in laboratory experiments, coefficients of friction (μ) of rocks are largely independent of the lithology and restricted to a narrow range of values between $\mu = 0.6$ and $\mu = 0.85$. These values seem applicable to many faults zones as well (Sibson, 1990, 1994). Based on this result, some investigations stress the role of pore fluid pressure as a condition for the reactivation of fault planes (Sibson, 1990, 1994, 2004). In this framework, the optimal faults for reactivation in compressional regimes will be those with a dip of 30°, and steeper fault planes would require fluid overpressure.

A compilation of fault plane dips for intracontinental reverse ruptures presents two distinct peaks: one corresponds to the optimal planes of 30° of dip, and the other is located around dips of 50° and would correspond to the inversion of normal faults (Sibson and Xie, 1998). In this way, the positive inversion of steep normal faults would require "fault-valve" behavior, with fluid pressure in the fault zone approaching lithostatic values, and rupturing followed by postseismic discharge (Sibson, 1990, 2004). At the "Byerlee" range of friction values, the angle of lockup for which fault inversion cannot take place is slightly less than 60° (Sibson and Xie, 1998; Sibson, 2004). However, as Byerlee (1978) stated, some fault gouges may lower the friction on natural faults considerably. Fault gouges form during fault slip in response to frictional wear of the wallrock. Wear processes include brittle shearing of asperities on all scales, asperity indentation and plowing, sidewall cracking and plucking, and progressive rock fragmentation and grain comminution by inter- and intra-granular cracking (Sibson, 1986). This leads initially to brecciation of the wallrock, and grain size as well as the degree of sorting in the breccia decrease with increasing displacement, generating gouges in large-displacement faults (Sibson, 1986). Wear processes also create pathways for fluid flow, and fluids may lead to alteration and neoformation of minerals in fault

zones through physico-chemical interaction with fault rocks and host rocks (Wibberley et al., 2008). The combination of these processes generates minerals which may lower the coefficient of friction of fault zones, depending on the composition of the gouge. For example, Morrow et al. (1992) report values between $\mu = 0.3$ and $\mu = 0.4$ for illite gouges and as low as $\mu = 0.2$ for montmorillonite gouges, and Moore and Lockner (2008) have shown that talc is extremely weak, with $\mu = 0.16$–0.23 at room temperature and even lower values at high temperatures (>100°). Collettini et al. (2009a) have obtained low coefficients of friction ($0.2 < \mu < 0.3$) for natural foliated fault zone rocks composed by a mixture of phyllosilicates. They also noted that the foliated fabric of the phyllosilicate network can be a major factor for fault zone weakening, producing low coefficients of friction even when small amounts of phyllosilicates are present in the fault zone. Presence of fluids seems to also lower the friction for minerals which adsorb water such as chrysotile, generating values of μ of the same order (Moore et al., 1997; Morrow et al., 2000). Another way of introducing low-friction material in fault zones can take place when a sedimentary succession containing shaly units is cut by a fault and these rocks are incorporated in the fault zone, leading to the formation of clay smears (Fisher and Knipe, 1998). In basement rocks, a "frictional-viscous" mechanism of deformation has been proposed based on the characteristics of large fault zones exhumed from depths >5 km, which present foliated cores comprising phyllonite and/or foliated cataclasite that overprint earlier random fabric cataclasites and brittle fractures (Imber et al., 2008). In this model, cataclasis acts during coseismic periods (high strain rate) and solution-precipitation aided cataclasis in the presence of a chemically active fluid may be operative during interseismic (low strain rate) periods (Chester and Higgs, 1992). These models predict significant (30–70%) weakening of faults that deform by frictional-viscous mechanisms compared with conventional crustal strength profiles based on Byerlee friction (Imber et al., 2008), and have been used to explain the continued reactivation of unfavorably and severely misoriented faults, such as the Zuccale low-angle normal fault in the isle of Elba (Collettini et al., 2009b) and the Median Tectonic Line in Japan (Imber et al., 2008).

All these processes may contribute to weaken fault zones with respect to wall rock, and would favor the reactivation of pre-existing faults over the generation of new structures.

3. Fault inversion modeling

The ReActiva software (Alaniz-Álvarez et al., 2000; Tolson et al., 2001) is a shareware product that calculates the orientation of planes amenable to reactivation under a given set of physical conditions. The user specifies the state of stress and the physical properties of the intact rock and the fault plane, and the program calculates the stress difference necessary to fracture the rock along the plane with the ideal orientation, and compares this value with that necessary for slip along pre-existing planes of weakness of certain orientation, as described by Alaniz-Álvarez et al. (1998). It is based on the equations of Yin and Ranalli (1992), who reformulated the Coulomb-Navier criteria for general crustal (non-Andersonian) conditions. The dependent variable in these equations is the stress difference ($\sigma_1 - \sigma_3$), instead of τ as used in the Mohr diagram. The effective stress field is calculated from the overburden pressure, modified with the pore fluid factor (λ) defined as the pore fluid pressure divided by the overburden pressure. Other variables used in the equations are the stress ratio $R = (\sigma_2 - \sigma_3)/(\sigma_1 - \sigma_3)$ and unit vectors normal to the fault (N_i) and to a horizontal plane (M_i), which allow the determination of slip planes in physical space. The Coulomb fracture criterion is then defined as:

$$(\sigma_1 - \sigma_3) = 2\mu\rho gz(1-\lambda) + 2c/\left(\mu^2+1\right)^{1/2} - \mu + 2\mu\left(M_1^2 + RM_2^2\right)$$

and the slip criterion as

$$(\sigma_1 - \sigma_3) = \mu_0\rho gz(1-\lambda_0) + c_0/\left[\left(N_1^2 + R^2N_2^2\right) - \left(N_1^2 + RN_2^2\right)^2\right]^{1/2} + \mu_0\left[\left(M_1^2 + RM_2^2\right) - \left(N_1^2 + RN_2^2\right)\right]$$

where g is the acceleration of gravity, z is depth, and λ_0 is the pore fluid factor for the pre-existing plane. Subscripts for N_i and M_i refer to the components of these vectors projected to the stress directions. For example $N_1 = N_i{}^*\cos\gamma_1$, where γ_1 is the angle between N_i and σ_1, $N_2 = N_i{}^*\cos\gamma_2$, where γ_2 is the angle between N_i and σ_2, etc.

In ReActiva, the results of the calculations are plotted as slip-rupture graphics, showing the poles of the reactivated planes on an equal area projection net. The advantages of the slip-rupture graphs technique were analyzed by Alaniz-Álvarez et al. (1998), who pointed out that relative to Mohr diagrams, the graphs have the advantage of working with geographic orientations of planes and principal stresses and it is not necessary to transform the data to a stress space. In some respects, the slip-rupture graphs are very similar to the slip tendency graphs introduced by Morris et al. (1996); however, the former allow predictions to be made regarding the possible reactivation of slip along planes with unfavorable orientations by varying different physical parameters. Furthermore, slip-rupture graphs address not only the possible reactivation of pre-existing planes of weakness as a function of the various parameters discussed above, but also the possibility of fracture. The implementation of this technique in ReActiva allows for the rapid calculation and visualization of results, which permits the evaluation of multiple scenarios by changing the parameters. Furthermore, the results are easily interpreted and can be transferred directly to natural examples.

4. The case study in the Malargüe FTB

4.1. The Mesozoic Neuquén basin and its major normal faults

The model of tectonic inversion in the Malargüe FTB proposes the reactivation of the normal faults which controlled the initial depocenters of the Neuquén basin, a retroarc basin developed during the Mesozoic (Fig. 1). The basin was filled with an alternance of marine and continental deposits controlled by the interaction of tectonics, sea level and volcanic activity in the magmatic arc, which allowed or restricted the connection with the paleo-Pacific Ocean (Legarreta and Uliana, 1996).

During the Late Triassic and Early Jurassic, extensional conditions prevailed in the retroarc of the South American subduction system, related to the breakup of the Gondwana supercontinent (Uliana and Biddle, 1988). In this setting, the beginning of subsidence in the Neuquén basin was controlled by normal faults which formed isolated hemigrabens and grabens (Charrier, 1979; Gulisano, 1981; Uliana and Biddle, 1988; Legarreta and Gulisano, 1989; Gulisano and Gutierrez Pleimling, 1995; Manceda and Figueroa, 1995; Legarreta and Uliana, 1996, 1999; Lanés, 2005; Vicente, 2005; Lanés et al., 2008; Giambiagi et al., 2009b; Bechis et al., 2009). A late Jurassic extensional reactivation has also been proposed for some areas of the basin including the present Andes of Mendoza (Cegarra and Ramos, 1996; Pángaro et al., 1996; Giambiagi

et al., 2003; Mescua et al., 2008). Orientations of the normal faults are very variable throughout the whole basin (Fig. 1), but in the northern sector (north of 36°S), strikes of the master faults vary between NNW and NNE (Giambiagi et al., 2009b). In the area corresponding to the Malargüe FTB, the major depocenters are from north to south: the Yeguas Muertas, Atuel, Río del Cobre, and Palauco depocenters (Fig. 1). Thickness of Mesozoic sedimentary deposits in these depocenters is in the order of thousands of meters, and locally exceeds 5.000 m. Within this succession, several units act as detachment layers due to their rheology: the Oxfordian gypsum (Auquilco Formation), the Tithonian to Berriasian black shales (Vaca Muerta Formation), and the Barremian to Aptian gypsum (Huitrín Formation).

4.2. The Malargüe FTB: general characteristics and proposed structural models

The Malargüe FTB can be divided latitudinally in two sectors: in the northern sector, in the inner (western) part of the belt the basement is involved, whereas the outer (eastern) sector presents a thin-skinned deformation, a feature shared with the southern sector of the Aconcagua FTB (Giambiagi et al., 2003). The southern sector, located south of the Salado river, has the basement involved in all its extension (Fig. 1).

The structural basement in this sector of the Andes is composed by Proterozoic low- to middle-grade metamorphics and Paleozoic low-grade schists and quartzites which crop out extensively to the north in the Cordillera Frontal (Polanski, 1964; Caminos, 1965) and Late Permian to Early Triassic acidic volcanics and plutons of the Choiyoi Group (Groeber, 1947), a unit of widespread regional distribution associated to extension during the beginning of the fragmentation of Gondwana (Llambías et al., 1993). These rocks underlie the Mesozoic sedimentary rocks of the fill of the Neuquén basin (see previous section). The basement crops out locally in the southern Malargüe FTB, associated to some faults and large anticlines, like in the Las Leñas block ("Dedos-Silla block" of Gerth, 1931) and along the Río Grande valley (Dimieri and Nullo, 1993; Kozlowski et al., 1993). In the northern Malargüe FTB, basement involvement in the inner sector is recognized because of the change in fold wavelengths and exposure level, from small folds with wavelength <1 km and outcrops of Cretaceous units in the east to folds with wavelengths >3–5 km and outcrops of Jurassic units in the west (Kozlowski et al., 1993; Mescua and Ramos, 2009). Throughout the fold-and-thrust belt, the basement structures transfer their displacement to the Mesozoic cover generating tight folds and thrusts with detachment levels in basinwide gypsum and shale units.

As explained in Introduction, different structural models have been proposed to account for the mechanism of basement deformation. We classify them as inversion, non-inversion and hybrid models. Inversion models were introduced because NW to NNE orientations of Mesozoic normal faults seem intuitively appropriate for reactivation in the Andean stress field (Manceda and Figueroa, 1995), whose major horizontal stress is oriented E–W (Somoza and Ghidella, 2005; Guzmán et al., 2007, 2009). The high angle of many of the reverse faults of the Malargüe FTB also suggests that the structures were originally normal faults. Later investigations provided other criteria to support that model: Ramos et al. (1996b) have shown that areas of basement-involved deformation in the High Andes of the provinces of San Juan and Mendoza coincide with extensional depocenters of the Neuquén basin, in contrast with areas of cover deformation, located where the syn-rift units of the basin where not deposited. In the northern Malargüe FTB, the change from basement involved to cover deformation corresponds to the Borbollón-La Manga lineament, which was interpreted as the main fault of the Atuel extensional depocenter on the basis of thickness and facies changes of the syn-extensional deposits on both sides of the lineament (Giambiagi et al., 2005, 2008a). The high angle of the La Manga fault is also pointed out by these authors as an argument for the interpretation of this structure as an inverted fault. These characteristics suggest a control on the location of basement-involved deformation by the extensional depocenters of the Neuquén basin. The lower shortening amount observed in basement-involved areas with respect to cover deformation areas (a feature obtained with all structural models) might be interpreted as a result of the inversion of high-angle faults in the former, since the high angle of the structures favors uplift over shortening (Ramos et al., 1996b). This fact, however, has been used as the main argument for non-inversion models (Dimieri et al., 1997). In the northern Malargüe FTB, the eastern sector of cover deformation presents high values of shortening which cannot be achieved through the transfer of shortening of inverted basement structures (Turienzo, 2010). This problem has been solved in two ways: applying non-inversion models (Turienzo, 2010) or hybrid models in which both inverted faults and new thrusts are responsible for shortening (Manceda and Figueroa, 1995; Giambiagi et al., 2003). Hybrid models have also been used for the structure of the southern Malargüe FTB (Giambiagi et al., 2009a) where some structures have been interpreted as inverted normal faults based on facies and thickness changes of Jurassic units between the foot wall and hanging wall blocks, and others with no evidence of inversion were interpreted as Andean basement thrusts.

5. Modeling results

In order to evaluate the inversion potential of the Mesozoic normal faults of the Malargüe FTB during the Andean orogeny, we carried out a set of calculations using ReActiva. Given the fact that physical conditions cannot be accurately determined for the case of study, we run several calculations varying the parameters in order to establish under which conditions a normal fault with a dip between 50° and 60° could be inverted. We calculated our models for a depth of 10 km, coincident with the depth of the main detachment for the Malargüe FTB interpreted from structural models (Manceda and Figueroa, 1995; Allmendinger et al., 2004; Giambiagi et al., 2009a) and seismological data (Farías et al., 2010). We assume that this is maximum depth for which inversion of the Mesozoic structures may have taken place; if a shallower depth is used for the models, the decrease in overburden pressure favors reactivation and the faults are inverted more easily (i.e. either the same faults are inverted with higher μ or lower λ, or more fault planes are inverted keeping all other parameters fixed). The stress state for the initial model was selected as reverse faulting with an R value of 0.5, which means that σ_2 has an intermediate value between σ_1 and σ_3. We started using the same values for the physical parameters of both the pre-existing fault and intact rock: a "Byerlee" value of $\mu = \mu_0 = 0.6$ for the coefficient of friction, a fluid pressure of $\lambda = \lambda_0 = 0.4$, and a cohesion of $c = c_0 = 30$ MPa (a value which is medium for metamorphic rocks and low for igneous rocks, Afrouz, 1992). In these conditions, no reactivation took place.

We proceeded to vary the parameters which can favor reactivation each at a time, and plotted the planes which were inverted (Fig. 3). In the first set of models, fluid pressure on the fault plane was increased using increments of 0.1. The second set of models consisted in varying the cohesion of the fault plane with a decrease of 5 MPa at each step. The third set of models was carried out decreasing the coefficient of friction on the plane, reducing 0.1 at each step. The total percentage of reactivated planes for each model was obtained and plotted in Fig. 3. Other variables were examined

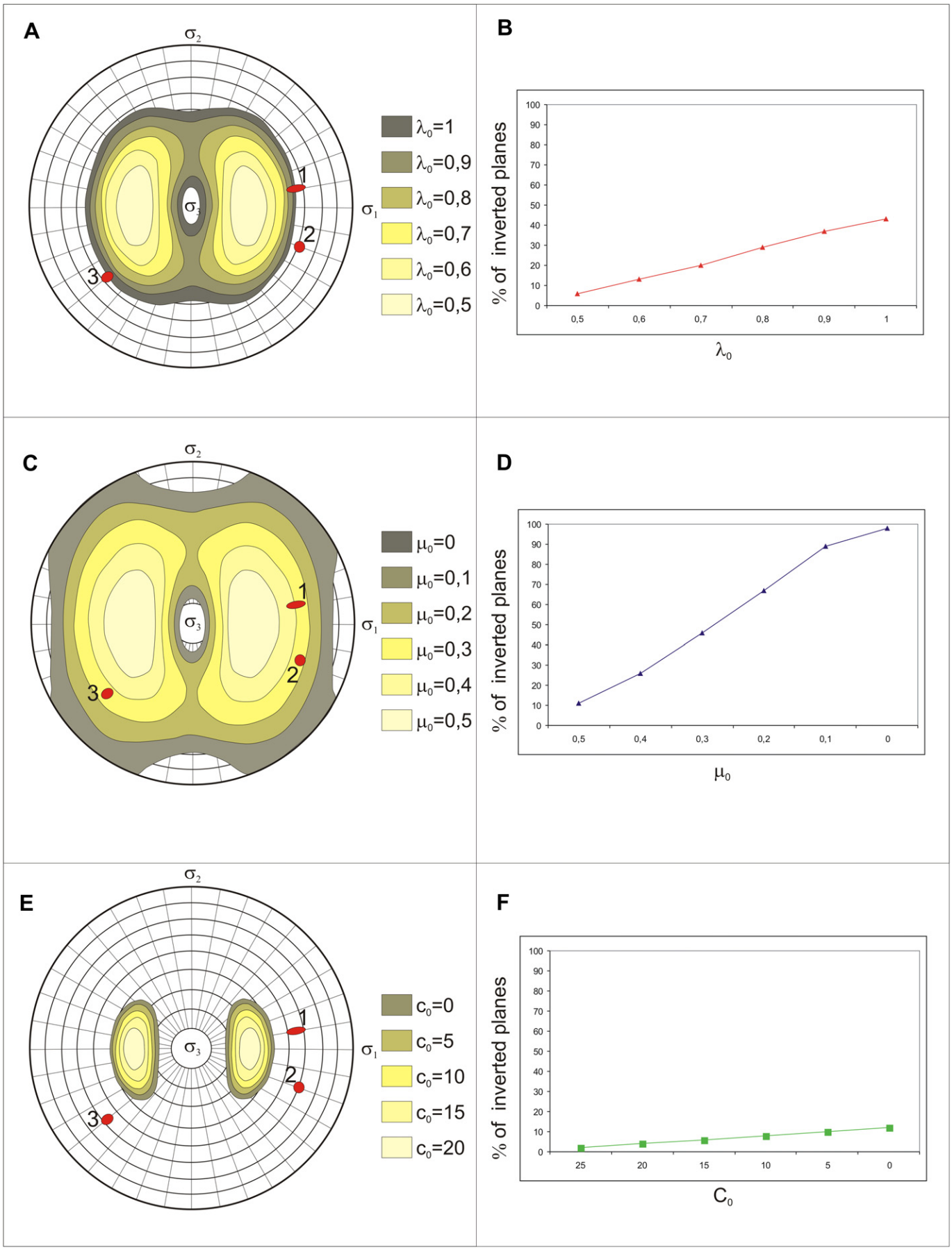
A
σ2
σ3
σ1
1
2
3
λ0=1
λ0=0,9
λ0=0,8
λ0=0,7
λ0=0,6
λ0=0,5
B
% of inverted planes
λ0
C
μ0=0
μ0=0,1
μ0=0,2
μ0=0,3
μ0=0,4
μ0=0,5
D
μ0
E
c0=0
c0=5
c0=10
c0=15
c0=20
F
C0

qualitatively, such as the variation of depth, the stress ratio R, and the density of rocks. The results were not significantly different for reasonable values of these parameters given our case of study, suggesting they are second-order controls, and will not be discussed in this work.

Our results show that the main factor controlling fault inversion is the coefficient of friction on the fault plane (Fig. 3C,D). A decrease of only 0.1 in this value ($\mu_0 = 0.5$) keeping all the other parameters fixed, readily produced the inversion of the most favorable planes, reactivating planes with maximum dips of 44° (11% of all planes). In the extreme case of frictionless fault planes ($\mu_0 = 0$), almost all pre-existing planes were reactivated (98% of all planes). For values of μ reported in the literature, like those for montmorillonite and talc gouges ($\mu_0 = 0.2$), 67% of the planes were reactivated. This included planes with maximum dips of 70°.

Keeping the value of $\mu = \mu_0 = 0.6$ fixed, the increase of pore fluid pressure on the fault plane was also able to produce inversion (Fig. 3A,B), but to a lesser extent than that obtained with a decrease in the coefficient of friction. With extremely high values of λ_0 ($\lambda_0 = 1$), only 43% of the planes were inverted, and maximum dip was 54°. This value is consistent with the lockup values of around 60° presented by Sibson and Xie (1998) and Sibson (2004) under similar conditions.

Cohesion seems to be the parameter with less influence for inversion. Variation of c_0 was quite ineffective to produce fault reactivation, with the inversion of only 12% of the pre-existing planes for a cohesionless fault plane ($c_0 = 0$). The maximum dip of reactivated planes was 43° (Fig. 3E,F). Increase of rock cohesion c was also modeled, but inversion of faults with dips of 50° could not be achieved even in cases of unrealistic values such as $c = 70$ MPa (and $c_0 = 0$ MPa).

6. Examples of suspected inverted faults from the Malargüe fold-and-thrust belt

6.1. The Río del Cobre fault

The Río del Cobre fault, located in the inner Malargüe FTB, has been interpreted as a Mesozoic normal fault which controlled deposition in the Río del Cobre depocenter (Mescua and Giambiagi, 2010). On the hanging wall of this structure, over 800 m of deep-sea Middle Jurassic deposits, and over 3.000 m of continental Late Jurassic (mostly Kimmeridgian) deposits crop out. On the foot wall, Middle Jurassic rocks do not crop out immediately east of the Río del Cobre fault but 7 km away where a Mesozoic basement high was developed. In this sector shallow marine deposits are found with less than 100 m of thickness. Late Jurassic rocks immediately east of the fault are 1.000 m thick. These facies and thickness changes are interpreted as the result of normal movement of the Río del Cobre fault during Mesozoic deposition.

At present, in the field, the Río del Cobre fault corresponds to a NNE trending, high angle (60°W) reverse fault zone with eastern vergence, whose trace extends for more than 10 km (Fig. 4). The fault zone has a maximum thickness of 600 m, and is composed of intensely strained and fractured red shales and gypsum of the Jurassic units found in the footwall of the fault surrounding fractured metric-scale blocks of sandstones of the Jurassic units of the hanging wall. An inverted (i.e., with reversed stratigraphy) block of the Jurassic units is found in the front of this sector of the fault zone (Fig. 4). A thermal spring found in the Río del Cobre valley is the result of the flow of deep water through the fault zone. Within the fault zone, calcite filled veins are frequent, some of them affected by small thrusts of centimetric displacement, which also evidences fluid flow and possibly overpressure in the fault zone. The displacement of the Río del Cobre fault is estimated at more than 3.000 m, based on the stratigraphic relations across the structure, which suggest a strong inversion according to the scale of Cooper et al. (1989). Toward the north and south the fault decreases its throw, giving place to large anticlines.

6.2. The La Manga fault

The Atuel depocenter is one of the most important initial depocenters of the Neuquén basin in the sector corresponding to the present Malargüe FTB, with a Late Triassic–Early Jurassic syn-extensional succession of more than 1.500 m (Bechis et al., 2009). It is the only depocenter where Late Triassic marine deposits are found (Riccardi et al., 1997), showing that a connection with the paleo-Pacific Ocean was established in this sector of the basin (Vicente, 2005). It has been proposed through sedimentary and structural investigations that the master fault of this depocenter was the La Manga fault (Lanés, 2005; Lanés et al., 2008; Giambiagi et al., 2005, 2008b, 2009b; Bechis et al., 2009). This structure corresponds to a 50 km long regional lineament of NNW trend, which marks the limit between basement-involved deformation to the west and cover deformation to the east in the northern sector of the Malargüe FTB (Fig. 1). Giambiagi et al. (2008a) present a structural model based on the interpretation of a seismic line, in which the La Manga fault is totally inverted transferring its shortening to the cover and including the generation of a hanging wall by-pass fault (Fig. 5). An alternative model was presented by Turienzo (2010), in which the La Manga fault corresponds to a newly created Andean thrust. In this model, no Mesozoic normal faults are taken into account, and the restitution of the cross-section presents continuous Late Triassic–Early Jurassic units across the La Manga fault, dismissing the existence of an extensional Atuel depocenter. It must be noted that balanced cross-sections constructed with both models arrive at similar values of shortening: 14.5 km (25%) and 13.7 km (23.3%), respectively. Following the evidence presented elsewhere for extensional tectonics during deposition in the Atuel depocenter, and for the La Manga fault as a major structure controlling its eastern border, in Section 7 we will evaluate if this structure could be inverted during Andean compressional deformation.

6.3. The Palauco fault

Inversion of east-dipping Mesozoic listric normal faults in the Palauco area was proposed by Manceda and Figueroa (1995). The coincidence of the Palauco anticline with a depocenter with over 1.000 m of syn-rift deposits was the base for their interpretation. In the model presented by these authors, only inversion of the low-angle sector of the normal faults took place, while shortcut and by-pass faults developed upwards. Giambiagi et al. (2009a) presented a compilation of the sub-surface information available for the Palauco area, and concluded that the Palauco fault is the result of the inversion of a series of NNW-trending en echelon Mesozoic

Fig. 3. Equal area plots of the results of ReActiva models. (A) Increase in pore fluid factor on pre-existing planes. Each color represents the inverted faults with increments of 0.1 in λ_0, from $\lambda_0 = 0.5$ to $\lambda_0 = 1$. All other parameters fixed (see text). (B) Percentage of planes inverted in each step of (A). (C) Decrease in the coefficient of friction on the pre-existing planes. Each color represents the inverted faults with a decrease of 0.1 of μ_0, from $\mu_0 = 0.5$ to $\mu_0 = 0$. All other parameters fixed. (D) Percentage of planes inverted in each step of (C). (E) Decrease in the cohesion on the pre-existing planes. Each color represents the inverted faults with a decrease of 5 MPa of c_0, from $c_0 = 20$ MPa to $c_0 = 0$ MPa. All other parameters fixed. (F) Percentage of planes inverted in each step of (E). The circles represent the planes corresponding to faults in the Malargüe fold-and-thrust belt: (1) La Manga fault: 350°, 50°–60°W; (2) Río del Cobre fault: 20°, 60°W; (3) Palauco fault, 140°, 60°E.

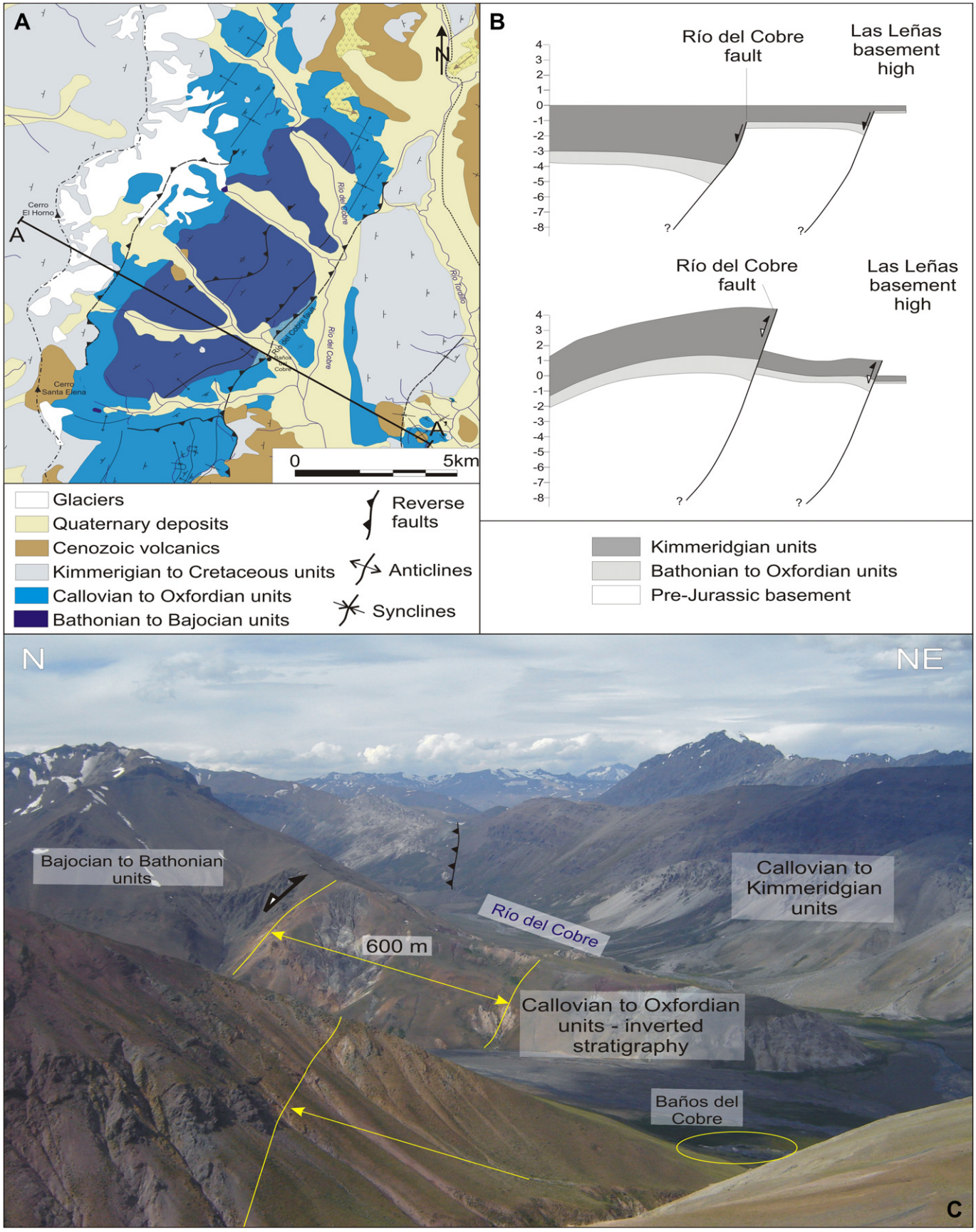

Fig. 4. (A) Geologic map of the Río del Cobre area. Location in Fig. 1. A–A′ is the trace of the schematic cross-section shown in Fig. 4B. (B) Pre-Andean geometry of the Río del Cobre depocenter, previous to the deposition of the marine Cretaceous units, and scheme showing the inversion of the Mesozoic normal faults. Location in Fig. 4A. (C) Photo of the 600 m thick reverse fault zone. Note the inverted block of Jurassic deposits in front of the fault zone and the associated thermal spring at Baños del Cobre. View to the NNE.

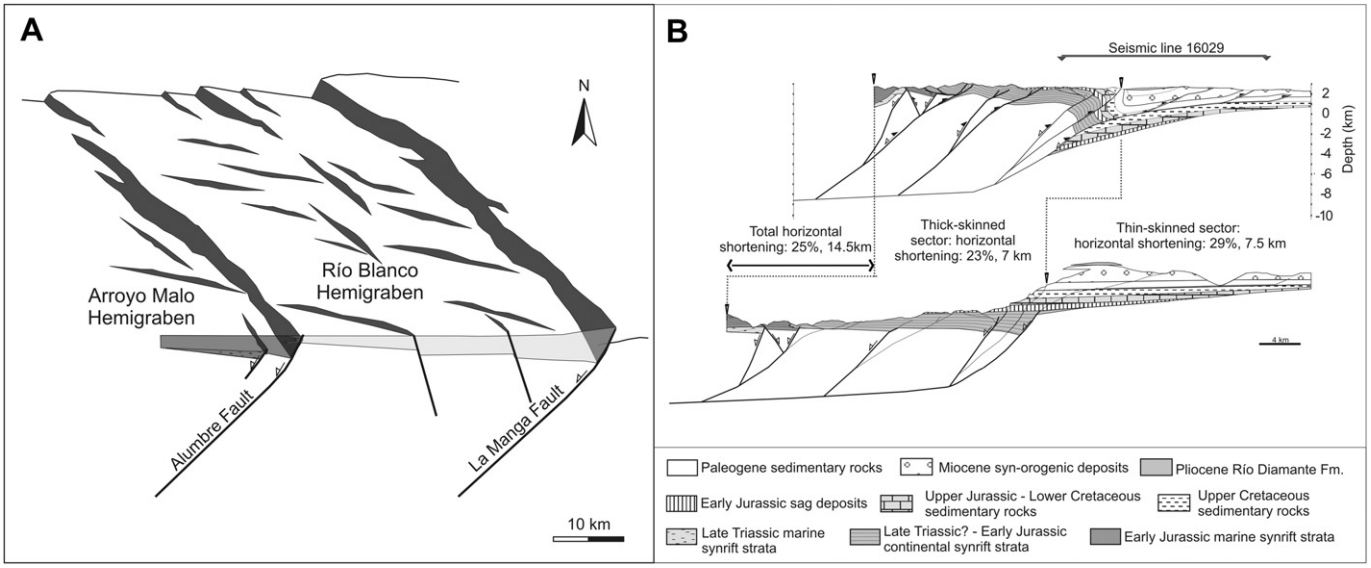

Fig. 5. (A) Geometry of the Atuel depocenter of the Neuquén basin, from Giambiagi et al. (2008a). (B) Balanced cross-section of the Malargüe FTB in the area of the Atuel depocenter of the Neuquén basin, from Giambiagi et al. (2008b). The structural model is based on the inversion of the La Manga fault. See location in Fig. 1.

normal fault segments. In the balanced cross-sections of Giambiagi et al. (2009a), both inversion of the whole Palauco fault and development of shortcut and by-pass faults are applied to resolve the geometry of the structures (Fig. 6).

7. Application of modeling in ReActiva to the faults of the Malargüe FTB

The main purpose of this work is to address the following question: under which conditions can the major Mesozoic normal faults of the Malargüe FTB be inverted during compressional tectonics? In order to obtain an answer, we will analyze the results of numerical modeling in ReActiva and compare these results with the characteristics of the three structures described in the previous section.

With the premises described in Section 4.2 for our models, the main results are that both NNE and NNW strikes are favorable for reactivation, and therefore the strike of the structures does not affect significantly the results in the studied case, and that for faults with a dip of 60°, a low coefficient of friction is a necessary condition (Fig. 3). Even increasing fluid pore pressure to very high values like $\lambda_0 = 1$, with a "Byerlee" coefficient of friction of $\mu_0 = 0.6$ inversion of fault planes with that angle does not take place: $\mu_0 = 0.5$ or lower is needed (Fig. 7). At low coefficients of friction, pore fluid pressure becomes irrelevant, and for $\mu_0 = 0.2$ no fluid overpressure is needed to invert a fault of 60° of dip.

Following these lines of reasoning, we will discuss next what values of μ_0 and λ_0 are possible in the Mesozoic normal faults of the Malargüe FTB. The decrease in μ_0 can be achieved in fault zones where clay gouges and/or smears have formed. Fault zone gauges form in mature faults with large displacements (Sibson, 1986). During the Mesozoic, the described faults had normal displacements in the order of several thousands of meters, as evidenced by the syn-rift deposits associated with the depocenters. Displacements of this order of magnitude should have produced significant wear of the wall rocks and fault gouges. Clay smears form when shaly units are cut by the fault and these rocks are included in the fault zone (Fisher and Knipe, 1998). The content of clay smear in a fault zone seems to be directly related to the content of shales in the sedimentary succession affected by the fault (Yielding, 2002). In our case of study, the upper part of the Mesozoic normal faults cut the sedimentary units of the Neuquén basin with important shale and evaporitic intervals which may contribute material for the formation of smears. For example in the Río del Cobre fault, red shales and gypsum of Jurassic units form part of the 600 m wide fault zone. These fault rocks probably lowered the friction coefficient of this segment of the fault zone. Therefore, a low μ_0 can be expected for parts of the high-angle segment of the fault zones in the 2 or 3 km closer to the surface. The sealing behavior of these fault rocks may also favor fluid overpressure (Fisher and Knipe, 1998). Exhumation levels in the Malargüe FTB prevent us from obtaining information about the development of the fault zones at greater depths. For faults developed in the metamorphic basement, if fault rocks such as clay gouges or phyllonites developed during Mesozoic normal displacements, the viscous-frictional mechanisms described in Section 3 may have acted to favor reactivation. In fact, according to Imber et al. (2008), the metamorphic conditions required for phyllonite development are likely to be met within the deeper parts of many, or even most, faults that cut continental basement rocks. The activation of frictional-viscous mechanisms would provoke a weakness of faults in the range of 30–70% of that expected with Byerlee friction values (Imber et al., 2008), which would create the conditions for inverting the major Mesozoic normal faults of the Malargüe FTB.

Fluid flow through many of the fault zones is evidenced at present by the existence of associated thermal springs, like in the Río del Cobre fault. If the fault zone was sealed in the past, fluid flow could have produced overpressure. This may have taken place for different causes: (i) shale and evaporitic units of the Neuquén basin fill may have acted as regional seals affecting the fault zones, as it happens at present in many oil traps in the area (Giampaoli et al., 2005; Legarreta et al., 2008); (ii) smears of the same lithologies incorporated in the fault zones may have limited flow within the fault zones acting as local seals (Fisher and Knipe, 1998); (iii) fluid-induced precipitation of minerals may also have contributed to closing the fluid pathways along the fault zones (Wibberley et al., 2008). All these processes would favor fault-valve behavior and reactivation of the Mesozoic normal faults. In addition to this, fluids could also have produced alteration in the fault zones, contributing to the formation of low-friction minerals, and to the decrease in the coefficient of friction.

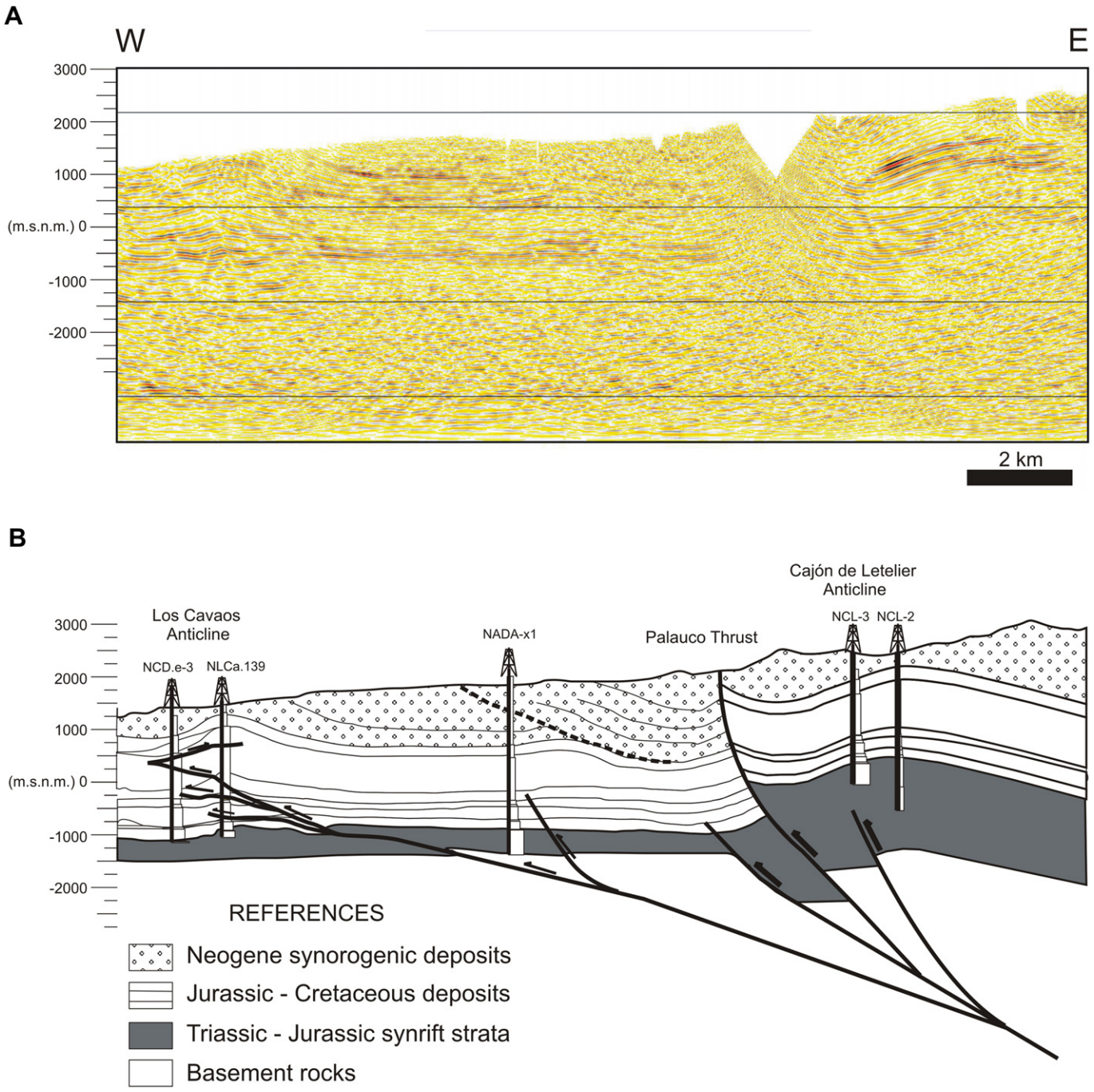

Fig. 6. (A) Seismic line and (B) structural interpretation of the Palauco fault, from Giambiagi et al. (2009a). Location in Fig. 1.

These facts suggest that re-use of the Mesozoic faults may have taken place if the conditions of low friction in the fault planes are met. A more detailed analysis is hindered in our case study by the limited exposure of the fault zones in the Malargüe FTB and the inherent heterogeneity of fault zones.

8. Discussion

Our results indicate that the Mesozoic normal faults of the initial depocenters of the Neuquén basin in the Malargüe FTB, specially those major structures representing the master faults of Triassic and Jurassic half-grabens, present characteristics which make them prone to reactivation in the Andean stress field, provided that:

(i) The fault planes present a low coefficient of friction, which implies the formation of clay gouges or some low-friction material in the fault zones or the activation of frictional-viscous mechanisms of fault weakening. The presence of fluids may also have contributed to fault inversion promoting the formation of low-friction minerals and creating over-pressure conditions.
(ii) The host rock presents typical physical characteristics: a “Byerlee” coefficient of friction, normal pore fluid pressure, and a standard value of cohesion.

We have analyzed the possible inversion of three of these structures, showing that given their orientations, inversion was

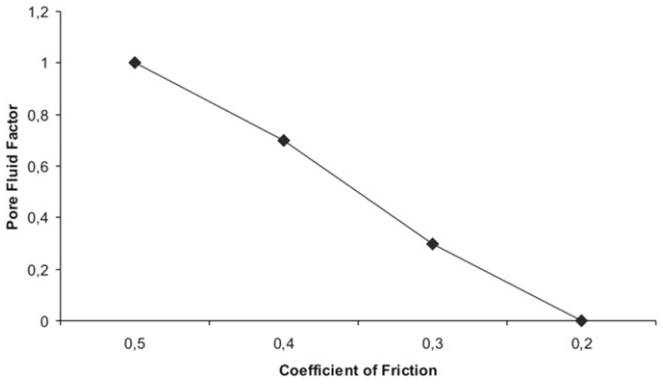

Fig. 7. Pore fluid pressure factor *vs.* coefficient of friction diagram, showing the combination of values for which a pre-existing fault of NNE to NNW strike and of 60° of dip is inverted.

possible with a combination of reasonable values of μ_0 and λ_0. Other faults for which inversion has been proposed (e.g. the Malargüe anticline, Giambiagi et al., 2009a) present similar characteristics to one of the modeled structures, implying that they have similar potential for inversion.

Our models were carried out for a depth of 10 km, the depth of the detachment of the fold-and-thrust belts during Andean deformation in this sector of the Andes (Manceda and Figueroa, 1995; Allmendinger et al., 2004; Giambiagi et al., 2009a; Farías et al., 2010). We used fault angles of 50°–60°, which are high angles typical of normal faults, and consistent with dips of structures observed at the surface or interpreted from seismic lines in the Malargüe FTB. Unfortunately, the deep geometry of the Mesozoic normal faults cannot be determined. A listric geometry is assumed, but the depth to the extensional detachment is unknown, which prevents us from reconstructing the variation of fault dip with depth. It can be deduced that at 10 km of depth the dip of the faults should be significantly lower than 60°, which makes our models "worst case scenarios". A smaller dip of the fault planes would make the orientation of the planes more favorable for reactivation, which would lead to inversion with lower λ_0 and/or higher μ_0. In fact, if the fault planes at 10 km of depth have a dip of 40°, either a value of $\mu_0 = 0.5$ or an increase in λ_0 up to 0.6 would suffice to produce inversion, with all other parameters fixed. Taking into account that, at present, fluid circulation along many of the faults produces thermal springs (e.g. the Río del Cobre fault), it can be deduced that if the structures were sealed from the surface previous to Andean compressional deformation, overpressure is likely to have occurred. Several Cretaceous units of the Neuquén basin may have acted as seals during the inversion, units which are now seals for hydrocarbon traps in the oilfields of the Neuquén basin: black shales (Vaca Muerta and Agrio Formations), and gypsum (Huitrín Formation) (Giampaoli et al., 2005; Legarreta et al., 2008). A value of $\lambda_0 = 0.6$ can be a reasonable expectation in this scenario. On the other hand, a low coefficient of friction can be expected for mature faults with thousands of meters of displacement, where fault gouges can develop. The activation of frictional-viscous mechanisms of fault weakening is a likely process to account for reactivation, and therefore inversion, of faults developed in basement rocks (Imber et al., 2008), and may also have taken place for the deeper part of the structures.

9. Concluding remarks

We conclude that the inversion of major Mesozoic normal faults during the Andean orogeny might have contributed significantly to uplift and deformation in the evolution of the Malargüe FTB. In the sectors of the fold-and-thrust belt where geological evidence shows the presence of important pre-existing faults related to the Mesozoic extensional episode, inversion must be taken into account in structural models of Andean deformation. As we have shown, given the orientation of these structures, the possible physical characteristics of fault planes and host rocks, and the Andean stress field, the Mesozoic normal faults are suitable for inversion. Features particular to each case will determine the mode of inversion, for example if only the re-use of the pre-existing fault takes place, or if shortcut or by-pass faults develop, or may locally inhibit inversion. But for the general cases, we have shown that inversion is expected to be the rule rather than the exception for the studied belt. Our results can be extended to other sectors of the Andes in which pre-existing crustal discontinuities with similar orientations are present and to other mountain belts with similar characteristics.

Acknowledgments

We would like to thank Susana Alaniz-Álvarez (UNAM) for kindly providing the updated link to download ReActiva. Comments by the journal reviewers, Dr. J. Kley and Dr. F. Hongn allowed us to improve this paper. Our work benefited of discussions with Florencia Bechis (CONICET) and Víctor A. Ramos (UBA). We acknowledge funding from CONICET (PIP 638 and PIP 5843) and the Agencia de Promoción Científica y Tecnológica (PICT 07-10942) to Giambiagi. This is a contribution to project IGCP 586-Y.

References

Afrouz, A.A., 1992. Practical Handbook of Mass Classification Systems and Modes of Ground Failure. CRC Press, Boca Raton.
Alaniz-Álvarez, S.A., Nieto-Samaniego, A.F., Tolson, G., 1998. A graphical technique to predict slip along a pre-existing plane of weakness. Engineering Geology 49, 53–60.
Alaniz-Álvarez, S.A., Nieto-Samaniego, A.F., Tolson, G., 2000. Assessing fault reactivation with the ReActiva program. Journal of Geoscience Education 48, 651–657.
Allmendinger, R.W., Zapata, T.R., Manceda, R., Dzelalija, F., 2004. Trishear kinematic modeling of structures with examples from the Neuquén Basin, Argentina. In: McClay, K.R. (Ed.), Thrust Tectonics and Hydrocarbon Systems. American Association of Petroleum Geologists, Memoir 82, Tulsa, pp. 356–371.
Anderson, E.M., 1951. The Dynamics of Faulting, second ed. Oliver and Boyd, Edimburgh.
Bechis, F., Giambiagi, L.B., Lanes, S., Garcia, V., Tunik, M., 2009. Evidencias de extensión oblicua en los depósitos de sinrift del sector norte de la cuenca Neuquina. Revista de la Asociación Geológica Argentina 65 (2), 293–310.
Bjorklund, T., Burke, K., 2002. Four-dimensional análisis of the inversion of a half-graben to form the Whittier fold-fault system of the Los Angeles basin. Journal of Structural Geology 24, 1369–1387.
Butler, R.W.H., Tavarnelli, E., Grasso, M., 2006. Structural inheritance in mountain belts: an Alpine–Apennine perspective. Journal of Structural Geology 28, 1893–1908.
Byerlee, J., 1978. Friction of rocks. Pure and Applied Geophysics 116, 615–626.
Caminos, R., 1965. Geología de la vertiente oriental del Cordón del Plata, Cordillera Frontal de Mendoza. Revista de la Asociación Geológica Argentina 20 (3), 351–392.
Carrera, N., Muñoz, J.A., Sàbat, F., Roca, E., Mon, R., 2006. The role of inversion tectonics in the structure of the Cordillera Oriental (NW Argentinean Andes). Journal of Structural Geology 28, 1921–1932.
Cegarra, M.I., Ramos, V.A., 1996. La faja plegada y corrida del Aconcagua. In: Ramos, V.A. (Ed.), Geología de la región del Aconcagua, provincias de San Juan y Mendoza. Dirección Nacional del Servicio Geológico, Subsecretaria de Minería de la Nación, Buenos Aires, pp. 387–422. Anales 24.
Charrier, R., 1979. El Triásico de Chile y regiones adyacentes de Argentina: una reconstrucción paleogeográfica y paleoclimática. Comunicaciones 26, 1–37.
Chester, F.M., Higgs, N.G., 1992. Multimechanism friction constitutive model for ultrafine quartz gouge at hypocentral conditions. Journal of Geophysical Research 97 (B2), 1859–1870.
Colletta, B., Hebrard, F., Letouzey, J., Werner, P., Rudkiewicz, J.L., 1990. Tectonic style and crustal structure of the Eastern Cordillera (Colombia) from a balanced cross-section. In: Letouzey, J. (Ed.), Petroleum and Tectonics in mobile belts. Editions Technip, Paris, pp. 81–100.
Collettini, C., Niemeijer, A., Viti, C., Marone, C., 2009a. Fault zone fabric and fault weakness. Nature 462, 907–911. doi:10.1038/nature08585.
Collettini, C., Holsworth, R.E., Smith, S.A.F., 2009b. Fault zone structure and deformation processes along an exhumed low-angle normal fault. Implications for

seismic behavior. In: Fukuyama, E. (Ed.), Fault Zone Properties and Earthquake Rupture Dynamics. International Geophysics Series, vol. 94, pp. 69–85.
Cooper, M.A., Williams, G.D., de Graziansky, P.C., Murphy, R.W., Needham, T., de Paor, D., Stoneley, R., Todd, S.P., Turner, J.P., Ziegler, P.A., 1989. Inversion tectonics – a discussion. In: Cooper, M.A., Williams, G.D. (Eds.), Inversion Tectonics. Geological Society, London, Special Publication Classics, pp. 335–347.
Dimieri, L.V., 1997. Tectonic wedge geometry at Bardas Blancas, Southern Andes (36°S), Argentina. Journal of Structural Geology 19 (11), 1419–1422.
Dimieri, L.V., Nullo, F.E., 1993. Estructura del frente montañoso de la Cordillera Principal (36° latitud sur), Mendoza. In: 12° Congreso Geológico Argentino y 2° Congreso de Exploración de Hidrocarburos, Actas 3, pp. 160–167.
Dimieri, L.V., Di Nardo, L., Frisicale, M., Delpino, S., Fortunatti, N., Nullo, F., 1997. Inversión tectónica: Un mecanismo ineficiente para producir acortamiento. In: 8° Congreso Geológico Chileno, Actas I, pp. 52–54.
Dewey, J.F., Bird, J.M., 1970. Mountain belts and the new global tectonics. Journal of Geophysical Research 75, 2625–2647.
Farías, M., Comte, D., Charrier, R., Martinod, J., David, C., Tassara, A., Tapia, F., Fock, A., 2010. Crustal-scale structural architecture in central Chile based on seismicity and surface geology: implications for Andean mountain building. Tectonics 29, TC3006. doi:10.1029/2009TC002480.
Fisher, Q.J., Knipe, R.J., 1998. Fault sealing processes in siliciclastic sediments. In: Jones, G., Fisher, Q.J., Knipe, R.J. (Eds.), Faulting, Fault Sealing and Fluid Flow in Hydrocarbon Reservoirs. Geological Society, London, Special Publications, vol. 147, pp. 117–134.
Gerth, E., 1931. La estructura geológica de la Cordillera Argentina entre los ríos Grande y Diamante en el sur de la provincia de Mendoza. Actas de la Academia Nacional de Ciencias 9 (1–2), 7–55. Córdoba.
Ghisetti, F.C., Sibson, R.H., 2006. Accommodation of compressional inversion in north-western South Island (New Zealand): old faults versus new? Journal of Structural Geology 28, 1994–2010.
Giambiagi, L.B., Alvarez, P., Godoy, E., Ramos, V.A., 2003. The control of preexisting extensional structures on the evolution of the southern sector of the Aconcagua fold and thrust belt, southern Andes. Tectonophysics 369, 1–19.
Giambiagi, L.B., Alvarez, P.P., Bechis, F., Tunik, M., 2005. Influencia de las estructuras de rift triásicas – jurásicas sobre el estilo de deformación en las fajas plegadas y corridas Aconcagua y Malargüe. Revista de la Asociación Geológica Argentina 60 (4), 661–671.
Giambiagi, L.B., Bechis, F., Lanés, S., Tunik, M., García, V., Suriano, J., Mescua, J.F., 2008a. Formación y evolución triásico-jurásica del depocentro Atuel, cuenca Neuquina, provincia de Mendoza. Revista de la Asociación Geológica Argentina 63 (4), 520–533.
Giambiagi, L.B., Bechis, F., García, V., Clark, A., 2008b. Temporal and spatial relationship between thick- and thin-skinned deformation in the Malargüe fold and thrust belt, southern Central Andes. Tectonophysics 459, 123–139.
Giambiagi, L., Ghiglione, M., Cristallini, E., Bottesi, G., 2009a. Kinematic models of basement/cover interactions: insights from the Malargüe fold and thrust belt, Mendoza, Argentina. Journal of Structural Geology 31, 1443–1457. doi:10.1016/j.jsg.2009.10.006.
Giambiagi, L.B., Tunik, M., Barredo, S., Bechis, F., Ghiglione, M., Alvarez, P., Drosina, M., 2009b. Cinemática de apertura del sector norte de la cuenca Neuquina. Revista de la Asociación Geológica Argentina 65 (1), 140–153.
Giampaoli, P., Ramírez, J.L., Gait, M.A., 2005. Estilos de entrampamiento en la faja plegada y corrida de Malargüe. In: Kozlowski, E., Vergani, G., Boll, A. (Eds.), Las trampas de hidrocarburos en las cuencas productivas de Argentina. IAPG, Simposio del 6° Congreso de Exploración y Desarrollo de Hidrocarburos, Buenos Aires, pp. 121–140.
Grier, M.E., Salfity, J.A., Allmendinger, R.W., 1991. Andean reactivation of the Cretaceous Salta rift, northwestern Argentina. Journal of South American Earth Sciences 4 (4), 351–372.
Groeber, P., 1947. Observaciones geológicas a lo largo del meridiano 70. 2. Hojas Sosneao y Maipo. Revista de la Asociación Geológica Argentina 2 (2), 141–176. Reprinted in Asociación Geológica Argentina, Serie C, Reimpresiones 1, Buenos Aires (1980).
Gulisano, C.A., 1981. El Ciclo Cuyano en el norte de Neuquén y sur de Mendoza. In: 8° Congreso Geológico Argentino, Actas 3, pp. 579–592.
Gulisano, C.A., Gutierrez Pleimling, A.R., 1995. Guía de Campo: El Jurásico de la Cuenca Neuquina. B) Provincia de Mendoza. In: Asociación Geológica Argentina, Serie E N°3 Buenos Aires.
Guzmán, C., Cristallini, E., Bottesi, G., 2007. Contemporary stress orientations in the Andean retroarc between 34° y 39°S from borehole breakout analysis. Tectonics 26, TC3016. doi:10.1029/2006TC001958.
Guzmán, C., Cristallini, E.O., 2009. Contemporary stress orientations from borehole breakout analysis in the southernmost flat-slab boundary Andean retroarc (32°44′ and 33° 40′ S). Journal of Geophysical Research. doi:10.1029/2007JB005505.
Helg, U., Burkhard, M., Caritg, S., Robert-Charrue, C., 2004. Folding and inversion tectonics in the Anti-Atlas of Morocco. Tectonics 23, TC4006. doi:10.1029/2003TC001576.
Homovc, J.F., Conforto, G.A., Lafourcade, P.A., Chelotti, L.A., 1995. Fold belt in the San Jorge basin, Argentina: An example of tectonic inversion. In: Buchanan, J.G., Buchanan, P.G. (Eds.), Basin Inversion. Geological Society, London, Special Publications, vol. 88, pp. 235–248.
Imber, J., Holdsworth, R.E., Smith, S.A.F., Jeffris, S.P., Collettini, C., 2008. Frictional-viscous flow, seismicity, and the geology of weak faults: a review and future directions. In: Wibberley, C.A.J., Kurz, W., Imber, J., Holdsworth, R.E., Colettini, C. (Eds.), The Internal Structure of Fault Zones: Implications for Mechanical and Fluid-Flow Properties. Geological Society, London, Special Publications, vol. 299, pp. 151–173.
Jaeger, J.C., 1969. Elasticity Fracture and Flow, third ed. Methuen & Co. Ltd., London.
Jaeger, J.C., Cook, N.G., 1979. Fundamentals of Rock Mechanics, third ed. Chapman & Hall, London.
Kley, J., Monaldi, C.R., Saltify, J.A., 1999. Along-strike segmentation of the Andean foreland: causes and consequences. Tectonophysics 301, 75–94.
Kley, J., Monaldi, C.R., 2002. Tectonic inversion in the Santa Bárbara system of the central Andean foreland thrust belt, northwestern Argentina. Tectonics 21 (6), 1061–1079. doi:10.1029/2002TC902003.
Kley, J., Rosello, E.A., Monaldi, C.R., Habighorst, B., 2005. Seismic and field evidence for selective inversion of Cretaceous normal faults, Salta rift, northwest Argentina. Tectonophysics 399, 155–172.
Kozlowski, E., Manceda, R., Ramos, V.A., 1993. Estructura. In: Ramos, V.A. (Ed.), Geología y Recursos Naturales de Mendoza, 12° Congreso Geológico Argentino y 2° Congreso de Exploración de Hidrocarburos, Relatorio, Buenos Aires, pp. 235–256,.
Lanés, S., 2005. Late Triassic to Early Jurassic sedimentation in northern Neuquén Basin, Argentina: Tectosedimentary evolution of the first transgression. Geologica Acta 3 (2), 81–106.
Lanés, S., Giambiagi, L., Bechis, F., Tunik, M., 2008. Late Triassic-Early Jurassic successions from the Atuel depocenter: depositional systems, sequence stratigraphy and tectonic controls. Revista de la Asociación Geológica Argentina 63 (4), 534–548.
Legarreta, L., Gulisano, C.A., 1989. Análisis estratigráfico secuencial de la cuenca Neuquina (Triásico superior- Terciario inferior). In: Chebli, G., Spalletti, L. (Eds.), Cuencas Sedimentarias Argentinas. Correlación Geológica Serie 6. Facultad de Ciencias Naturales, Universidad Nacional de Tucumán, Tucumán, pp. 221–243.
Legarreta, L., Uliana, M.A., 1996. The Jurassic succession in west-central Argentina: stratal patterns, sequences and paleogeographic evolution. Palaeogeography, Palaeoclimatology, Palaeoecology 120, 303–330.
Legarreta, L., Uliana, M.A., 1999. El Jurásico y Cretácico de la Cordillera Principal y la cuenca Neuquina. 1. Facies sedimentarias. In: Caminos, R. (Ed.), Geología Argentina, Servicio Geológico y Minero Argentino. Instituto de Geología y Recursos Minerales, Buenos Aires, pp. 399–416. Anales 29(16).
Legarreta, L., Villar, H.J., Cruz, C.E., Laffitte, G.A., Varadé, R., 2008. Revisión integrada de los sistemas generadores, estilos de migración-entrampamiento, y volumetría de hidrocarburos en los distritos productivos de la cuenca Neuquina, Argentina. In: Cruz, C.E., Rodríguez, J.F., Hechern, J.J., Villar, H.J. (Eds.), Sistemas Petroleros de las Cuencas Andinas. Instituto Argentino del Petróleo y el Gas, Buenos Aires, pp. 79–108.
Lisle, R.J., Srivastava, D.C., 2004. Test of the frictional reactivation theory for faults and validity of fault slip analysis. Geology 32, 569–572.
Llambías, E.J., Kleiman, L.E., Salvarredi, J.A., 1993. El magmatismo gondwánico. In: Ramos, V.A. (Ed.), Geología y Recursos Naturales de Mendoza, 12° Congreso Geológico Argentino y 2° Congreso de Exploración de Hidrocarburos, Relatorio, Buenos Aires, pp. 53–64.
Manceda, R., Figueroa, D., 1995. Inversion of the Mesozoic Neuquen rift in the Malargüe fold-thrust belt, Mendoza, Argentina. In: Tankard, A.J., Suarez, R., Welsink, H.J. (Eds.), Petroleum Basins of South America. American Association of Petroleum Geology, Memoirs 62, Tulsa, pp. 369–382.
Mescua, J.F., Giambiagi, L.B., Bechis, F., 2008. Evidencias de tectónica extensional en el Jurásico tardío (Kimeridgiano) del suroeste de la provincia de Mendoza. Revista de la Asociación Geológica Argentina 63 (4), 512–519.
Mescua, J.F., Ramos, V.A., 2009. Estratigrafía y estructura de las nacientes del río Borbollón, alto río Diamante, provincia de Mendoza. Revista de la Asociación Geológica Argentina 65 (1), 111–122.
Mescua, J.F., Giambiagi, L.B., 2010. The deep-sea deposits of the Cuyo Group in the Río del Cobre depocenter, Mendoza, Argentina: characteristics and paleogeographic implications. In: 18° International Sedimentological Congress, Abstracts Volume, Mendoza, p. 601.
Moore, D.E., Lockner, D.A., 2008. Talc friction in the temperature range 25°–400 °C: relevance for fault zone weakening. Tectonophysics 449, 120–132.
Moore, D.E., Lockner, D.A., Shengli, M., Summers, R., Byerlee, J.D., 1997. Strengths of serpentine gouges at elevated temperatures. Journal of Geophysical Research 102, 14787–14801.
Morley, C.K., Haranya, C., Phoosongsee, W., Pongwapee, S., Kornsawan, A., Wonganan, N., 2004. Activation of rift parallel pre-existing fabrics during extension and their effect on deformation style: examples from the rifts of Thailand. Journal of Structural Geology 26, 1803–1829.
Morris, A., Ferrill, D.A., Henderson, D.B., 1996. Slip-tendency analysis and fault reactivation. Geology 24, 275–278.
Morrow, C., Radney, B., Byerlee, J.D., 1992. Frictional strength and the effective pressure law of montmorillonite and illite clays. In: Evans, B., Wong, T. (Eds.), Fault Mechanics and Transport Properties of Rocks. Academic Press, pp. 69–88.
Morrow, C., Moore, D.E., Lockner, D.A., 2000. The effect of mineral bond strength and adsorbed water on fault gouge frictional strength. Geophysical Research Letters 7, 815–818.
Mouthereau, F., Lacombe, O., 2006. Inversion of the Paleogene Chinese continental margin and thick-skinned deformation in the western foreland of Taiwan. Journal of Structural Geology 28, 1977–1993.
Pángaro, F., Ramos, V.A., Godoy, E., 1996. La faja plegada y corrida de la Cordillera Principal de Argentina y Chile a la latitud del Cerro Palomares (33°35′S). In: 13° Congreso Geológico Argentino y 3° Congreso Exploración de Hidrocarburos, Actas 2, Buenos Aires, pp. 315–324.

Polanski, J., 1964. Descripción Geológica de la Hoja 25a -Volcán San José, Provincia de Mendoza. Boletín N° 98. Dirección Nacional de Geología y Minería, Buenos Aires.
Ramos, V.A., Aguirre-Urreta, M.B., Alvarez, P.P., Cegarra, M.I., Cristallini, E.O., Kay, S.M., Lo Forte, G.L., Pereyra, F.X., Pérez, D.J., 1996a. Geología de la región del Aconcagua, provincias de San Juan y Mendoza. Dirección Nacional del Servicio Geológico, Subsecretaría de Minería de la Nación, Buenos Aires. Anales 24.
Ramos, V.A., Cegarra, M., Cristallini, E., 1996b. Cenozoic tectonics of the High Andes of west-central Argentina. Tectonophysics 259, 185–200.
Ramos, V.A., Alemán, A., 2000. Tectonic evolution of the Andes. In: Cordani, U.G., Milani, E.J., Thomaz Filho, A., Campos, D.A. (Eds.), 31 International Geological Congress, Río de Janeiro. Tectonic Evolution of South America, pp. 635–685.
Ramsay, J.G., 1967. Folding and Fracturing of Rocks. McGraw-Hill, New York.
Riccardi, A., Damborenea, S.E., Manceñido, M.O., Scasso, R., Lanés, S., Iglesia Llanos, M.P., Stipanicic, P.N., 1997. Primer registro de Triásico marino fosilífero de la Argentina. Revista de la Asociación Geológica Argentina 52, 228–234.
Rutter, E.H., Holdsworth, R.E., Knipe, R.J., 2001. The nature and significance of fault zone weakening: an introduction. In: Holdsworth, R.E., Strachan, R.A., Macloughlin, J.F., Knipe, R.J. (Eds.), The Nature And Significance of Fault Zone Weakening. Geological Society, London, Special Publications, vol. 186, pp. 1–11.
Sibson, R.H., 1977. Fault rocks and fault mechanisms. Journal of the Geological Society 133, 191–213.
Sibson, R.H., 1985. A note on fault reactivation. Journal of Structural Geology 7, 751–754.
Sibson, R.H., 1986. Brecciation processes in fault zones: inferences from earthquake rupturing. Pure and Applied Geophysics 124, 159–176.
Sibson, R.H., 1990. Rupture nucleation on unfavorably oriented faults. Bulletin of the Seismological Society of America 80, 1580–1604.
Sibson, R.H., 1994. An assessment of field evidence for “Byerlee” friction. Pure and Applied Geophysics 142, 645–662.
Sibson, R.H., 2004. Frictional mechanics of seismogenic thrust systems in the upper continental crust—implications for fluid overpressures and redistribution. In: McClay, K.R. (Ed.), Thrust Tectonics And Hydrocarbon Systems. American Association of Petroleum Geologists, Memoir 82, Tulsa, pp. 1–17.
Sibson, R.H., Xie, G., 1998. Dip range for intracontinental reverse fault ruptures: Truth not stranger than fiction? Bulletin of the Seismological Society of America 88, 1014–1022.
Somoza, R., Ghidella, M.E., 2005. Convergencia en el margen occidental de América del Sur durante el Cenozoico: subducción de las placas de Nazca, Farallón y Aluk. Revista de la Asociación Geológica Argentina 60 (4), 797–809.
Tolson, G., Alaniz-Alvarez, S.A., Nieto-Samaniego, A.F., 2001. ReActiva 2.4, A Plotting Program to Calculate the Potential of Reactivation of Preexisting Planes of Weakness. Instituto de Geología, Universidad Nacional Autónoma de México. Available at: http://www.geologia.unam.mx/igl/index.php?option=com_content&view=category&layout=blog&id=136&Itemid=93 (last accessed 19.07.11).
Turienzo, M.M., 2010. Structural style of the Malargüe fold-and-thrust belt at the Diamante river area (34°30′S–34°50′S) and its linkage with the Cordillera Frontal, Andes of Central Argentina. Journal of South American Earth Sciences 29, 537–556.
Uliana, M., Biddle, K., 1988. Mesozoic-Cenozoic paleogeographic and geodynamic evolution of southern South America. Revista Brasileira de Geociencias 18 (2), 172–190.
Uliana, M., Arteaga, M., Legarreta, L., Cerdan, J., Peroni, G., 1995. Inversion structures and hydrocarbon occurrence in Argentina. In: Buchanan, J.G., Buchanan, P.G. (Eds.), Basin Inversion. Geological Society, London, Special Publications, vol. 88, pp. 211–233.
Underhill, J.R., Paterson, S., 1998. Genesis of tectonic inversion structures: seismic evidence for the development of key structures along the Purbeck-Isle of Wight disturbance. Journal of the Geological Society 155, 975–992.
Vicente, J.C., 2005. Dynamic paleogeography of the Jurassic Andean Basin: pattern of transgression and localisation of main straits through the magmatic arc. Revista de la Asociación Geológica Argentina 60 (1), 221–250.
Wibberley, C.A.J., Yielding, G., Di Toro, G., 2008. Recent advances in understanding of fault zone internal structure: a review. In: Wibberley, C.A.J., Kurz, W., Imber, J., Holdsworth, R.E., Collettini, C. (Eds.), The Internal Structure of Fault Zones: Implications for Mechanical and Fluid-Flow Properties. Geological Society, London, Special Publication, vol. 299, pp. 5–33.
Williams, G.D., Powell, C.M., Cooper, M.A., 1989. Geometry and kinematics of inversion tectonics. In: Cooper, M.A., Williams, G.D. (Eds.), Inversion Tectonics. Geological Society, London, Special Publication Classics, pp. 3–15.
Yielding, G., 2002. Shale gouge ratio – calibration by geohistory. In: Koestler, A.G., Hunsdale, R. (Eds.), Hydrocarbon Seal Quantification. Norwegian Petroleum Society, Amsterdam, Special Publications, vol. 11, pp. 1–15.
Yin, Z.M., Ranalli, G., 1992. Critica1 stress difference, fault orientation and slip direction in anisotropic rocks under non-Andersonian stress systems. Journal of Structural Geology 14, 237–244.
Zanchi, A., Berra, F., Mattei, M., Ghassemi, M.R., Sabouri, J., 2006. Inversion tectonics in central Alborz, Iran. Journal of Structural Geology 28, 2023–2037.